Monthly Notices
of the
ROYAL ASTRONOMICAL SOCIETY

Mon. Not. R. Astron. Soc. **419,** 3258–3267 (2012) doi:10.1111/j.1365-2966.2011.19966.x

Revisiting the proposed planetary system orbiting the eclipsing polar HU Aquarii

Robert A. Wittenmyer,[1⋆] J. Horner,[1] J. P. Marshall,[2] O. W. Butters[3] and C. G. Tinney[1]

[1]*Department of Astrophysics and Optics, School of Physics, University of New South Wales, Sydney 2052, Australia*
[2]*Departmento Física Teórica, Facultad de Ciencias, Universidad Autónoma de Madrid, Cantoblanco, 28049 Madrid, España*
[3]*Department of Physics and Astronomy, University of Leicester, Leicester LE1 7RH*

Accepted 2011 October 6. Received 2011 October 5; in original form 2011 September 1

ABSTRACT

It has recently been proposed, on the basis of eclipse-timing data, that the eclipsing polar cataclysmic variable HU Aquarii is host to at least two giant planets. However, that result has been called into question based upon the dynamical stability of the proposed planets. In this work, we present a detailed re-analysis of all eclipse-timing data available for the HU Aquarii system, making use of standard techniques used to fit orbits to radial-velocity data. We find that the eclipse timings can be used to obtain a two-planet solution that does not require the presence of additional bodies within the system. We then perform a highly detailed dynamical analysis of the proposed planetary system. We show that the improved orbital parameters we have derived correspond to planets that are dynamically unstable on unfeasibly short time-scales (of the order of 10^4 yr or less). Given these results, we discuss briefly how the observed signal might in fact be the result of the intrinsic properties of the eclipsing polar, rather than being evidence of dynamically improbable planets. Taken in concert, our results highlight the need for caution in interpreting such timing variations as being planetary in nature.

Key words: planets and satellites: dynamical evolution and stability – binaries: close – binaries: eclipsing – stars: individual: HU Aqr – planetary systems – white dwarfs.

1 INTRODUCTION

Cataclysmic variables (CVs) are interacting binary stars composed of a white dwarf primary and a Roche lobe filling M dwarf secondary. In the case of HU Aqr, an AM Her class CV, the material being accreted by the primary from the secondary is channelled along an accretion stream by the white dwarf's magnetic field. A comprehensive overview of these systems can be found in Hellier (2001). Such systems are known to exhibit quasi-periodic variations in their photometry. A number of factors can contribute to those variations, with well-accepted causes including the level of activity of the secondary (star spots and associated stellar cycles) and also that star's shape.

A number of recent studies have suggested that certain CVs host planetary-mass companions. As the postulated planetary companions orbit the central stars, they cause those stars to move back and forth as they orbit around the system's centre of mass. As a result, the distance between the Earth and the host stars varies as a function of time, meaning that the light from the stars must sometimes travel further to reach us than at other times. This effect results in measurable variations in the timing of mutual eclipse events between the two stars that can be measured from the Earth. Using this method, planetary-mass companions have recently been announced around the CVs UZ For (Potter et al. 2011), NN Ser (Beuermann et al. 2010), DP Leo (Qian et al. 2010) and HU Aqr (Qian et al. 2011). In each of these studies, the eclipse timings are first fitted to a linear ephemeris. The residuals from this ephemeris (the O − C or observed−calculated timings) are then plotted and found to show further, higher order variations. These O − C timings can then be fitted with one or more superposed Keplerian orbits in a manner essentially identical to that employed in Doppler radial-velocity planet detection. In Horner et al. (2011), we used the methodology of Marshall, Horner & Carter (2010) to simulate the long-term dynamical stability of the two giant planets proposed as orbiting HU Aqr (Qian et al. 2011). We showed that the nominal two-planet solution was extremely unstable on short time-scales ($\sim 10^5$ yr), unless the outer planet orbited in a retrograde and coplanar sense relative to the inner (i.e. with the two planetary orbits inclined by 180° to each other). Given that such a configuration seems highly unlikely, we suggested that either the system is currently undergoing a dynamical re-arrangement (also highly improbable given the $\gtrsim 10^9$ yr age of the post-main-sequence primary), or that the system is significantly different from that proposed by Qian et al. (2011).

In this work, we apply the standard statistical methods used by the radial-velocity planet search community to the timing data for

⋆E-mail: rob@phys.unsw.edu.au

Table 1. Eclipse timing residuals for HU Aqr.

JD − 240 0000	O − C (s)	Uncertainty (s)
49 217.436 369	−22.2	1.0
49 217.523 190	−23.1	1.0
49 217.610 010	−22.6	1.0
49 217.696 830	−19.8	2.0
49 218.651 855	−21.2	2.0
49 218.738 675	−20.4	2.0
49 221.603 749	−21.4	2.0
49 221.690 569	−21.6	2.0
49 221.777 389	−20.9	2.0
50 325.959 283	−2.5	2.4
50 326.046 103	−2.5	2.4
50 338.895 523	−3.7	2.4
50 285.414 154	−4.3	10.0
50 285.500 975	−8.3	10.0
50 286.455 999	−9.4	10.0
50 328.390 254	6.0	10.0
50 328.477 074	7.6	10.0
50 330.387 123	−7.1	10.0
50 330.473 944	−6.7	10.0
51 081.383 615	8.3	10.0
51 481.278 394	20.9	2.0
51 703.625 447	22.3	7.0
51 704.580 472	20.1	7.0
52 145.367 661	22.8	4.0
51 703.625 447	22.3	8.0
51 704.580 472	20.1	8.0
51 821.440 735	24.7	1.0
51 821.527 555	24.7	1.0
51 350.874 147	15.1	1.0
51 353.826 041	15.4	1.0
51 354.867 886	16.6	1.0
51 731.494 797	23.5	1.0
51 731.581 617	23.7	1.0
52 174.278 855	20.9	1.0
52 174.365 676	21.1	1.0
52 411.559 018	14.9	1.0
52 552.381 713	11.3	1.0
52 553.336 737	8.9	1.0
52 787.665 007	3.0	1.0
52 789.575 056	1.7	1.0
53 205.444 789	−6.8	1.5
53 205.531 609	−7.1	1.5
53 209.525 348	−6.0	1.5
53 212.564 062	−5.7	1.5
53 293.307 038	−7.6	1.5
53 295.303 907	−9.2	1.5
53 296.258 931	−7.5	1.5
53 299.297 645	−7.6	1.5
53 533.539 094	−6.8	1.5
53 918.500 764	−4.8	1.5
53 925.446 396	−4.9	1.5
54 320.479 233	1.5	1.5
54 320.566 053	−0.3	1.5
52 411.211 737	11.6	5.0
52 779.937 991	3.7	5.0
52 411.385 378	16.8	2.0
52 411.385 378	17.3	2.0
52 411.472 198	16.8	2.0
52 413.642 708	12.3	1.0
52 414.684 553	16.2	1.0
52 783.671 268	2.6	1.0
53 504.888 361	−5.8	0.5
53 505.843 386	−5.9	0.5
53 505.930 206	−5.8	0.5
53 506.798 410	−5.9	0.5
53 506.885 230	−5.9	0.5
53 507.927 075	−5.8	0.5
54 270.817 962	2.4	1.4
54 270.904 782	2.6	1.4
54 273.769 856	2.5	1.4
54 273.856 676	2.4	1.4
54 972.326 823	−2.9	3.4
55 086.061 552	−6.5	3.4
55 087.103 397	−4.1	3.4
55 122.005 199	−4.7	3.4
55 136.070 104	−4.1	3.4
55 162.984 429	−7.5	3.4
55 164.026 274	−7.0	3.4
55 164.981 299	−9.0	3.4
55 172.968 776	−9.0	3.4
55 335.322 931	−14.6	3.4

HU Aqr given by Qian et al. (2011). Section 2 briefly describes the observational data used for our analysis. In Section 3, we detail the analysis methods applied to these data, and the resulting planetary system configurations implied. In Section 4, we discuss the dynamical implications of our results, before exploring possible alternatives to the planet hypothesis in Section 5.

2 OBSERVATIONAL DATA

Following the discovery paper by Qian et al. (2011), we make use of the same 82 O−C eclipse egress times (Table 1), consisting of 72 data points from the literature (Schwarz et al. 2009) and 10 new timings presented by Qian et al. (2011). All eclipse timings have been fitted with a linear ephemeris given by

$$244\,9102.920\,257 + 0.086\,829\,4936E. \quad (1)$$

The residuals from the fit to this linear ephemeris are plotted in Fig. 1. The root-mean-square (rms) scatter in the timing data is 13.4 s, and the reduced χ^2 of the linear ephemeris is quite large at 108.6. There are significant deviations from the linear ephemeris, suggestive of additional perturbing bodies which result in periodic eclipse-timing variations. We therefore proceed with fitting Keplerian orbits to these signals.

3 ORBIT FITTING

In this section, we detail the orbit-fitting process for two cases. First, in Section 3.1, we follow Qian et al. (2011), and consider the data after the removal of a quadratic trend. In Section 3.2, we attempt to fit the data without removing a quadratic trend. It is well accepted that in fitting radial-velocity data (to which results on eclipse timing are clearly analogous), if a long-period object is suspected, the removal of a quadratic trend from the data is not ideal. The physically meaningful function to fit and remove is a Keplerian (if the variation is thought to be due to planetary orbits). As the Keplerian function is a complex one, and not necessarily well approximated by a quadratic, it is both preferable and more rigorous to attempt to fit a Keplerian orbit – even if the parameters so derived are not well constrained, one will at least not introduce spurious signals due to a poor match between a quadratic and a Keplerian.

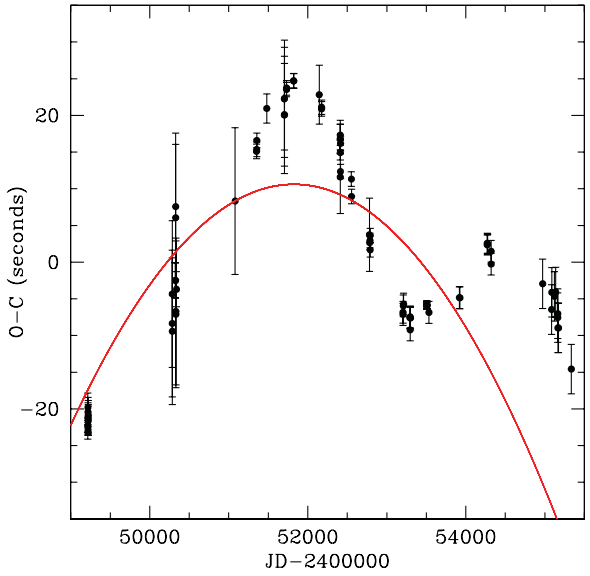

Figure 1. O − C eclipse timings for HU Aqr, after fitting a linear ephemeris (given by equation 1). A quadratic fit to these data is overplotted as a solid line. The data are those used in Qian et al. (2011), which include 72 observations initially presented by Schwarz et al. (2009). At least one sinusoidal variation is evident, suggesting the presence of at least one additional perturbing body.

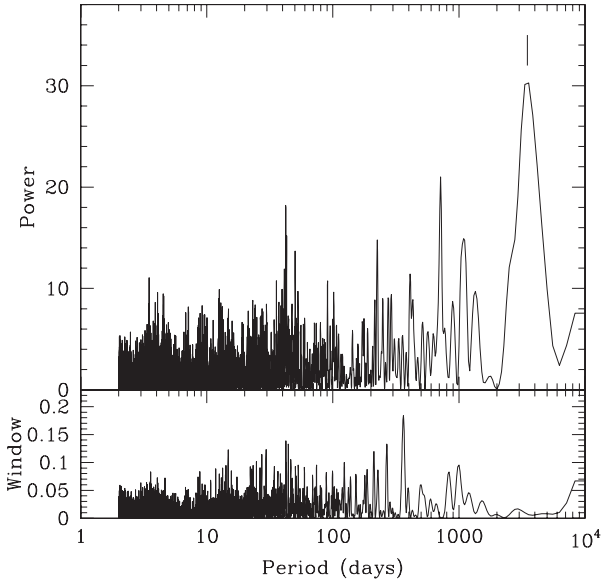

Figure 2. Periodogram of the O − C timing data for HU Aqr, using raw data (residuals from a linear ephemeris) with quadratic trend also removed. A strong signal is evident near 3500 days.

3.1 Removing a quadratic trend

In order to test the results of Qian et al. (2011), we match their approach by fitting Keplerian orbits after removing a long-term quadratic trend. First, we fit a quadratic trend to the original timing data; the fitted parameters are

$$(\mathrm{O}-\mathrm{C}) = (-4.1 \times 10^{-6})(\mathrm{JD})^2 + 0.43(\mathrm{JD}) - 1.10 \times 10^4, \qquad (2)$$

where JD is the observation date in the form (Julian Date − 240 0000). Then, we fit a single planet (model A1). A standard Lomb–Scargle periodogram (Lomb 1976; Scargle 1982) shows a clear signal near 3500 days (Fig. 2). We fit a Keplerian orbit model using GaussFit (Jefferys, Fitzpatrick & McArthur 1987). The single-planet solution is given in Table 2 as 'model A1'. The residuals to the one-planet fit are shown in Fig. 3, as is the periodogram of those residuals. After removing the dominant periodicity, there is a significant peak at $\gtrsim$8000 d. Using the bootstrap randomization method described by Kürster et al. (1997), this peak is found to have a false-alarm probability (FAP) of <0.01 per cent (10 000 bootstraps). Owing to the high significance of this residual peak, and the large rms of the one-planet residuals (6.57 s: Table 2), we proceed by fitting a second planet.

Given the substantial uncertainty in the system parameters, we used a genetic algorithm to explore a wide parameter space (e.g. Cochran et al. 2007; Tinney et al. 2011). The initial range of orbital periods supported by these data were first estimated by the periodogram analysis described above. The parameters of the best two-planet solution obtained by the genetic algorithm were then used as initial inputs for the GaussFit least-squares fitting procedure used above. The two-planet fit and a periodogram of its residuals are shown in Fig. 4. The parameters of the two-planet fit are given in Table 2 as 'model A2'. Since the total duration of the data set is 6118 days, and the best-fitting period for an outer body is

Table 2. Orbital solutions for HU Aquarii.

Model	Parameter	Inner planet	Outer planet
A1	Orbital period (d)	3538 ± 54	
	Amplitude (s)	12.5 ± 0.8	
	Eccentricity	0.26 ± 0.05	
	ω (°)	171 ± 12	
	T_0 (JD − 240 0000)	$53\,092 \pm 517$	
	Orbital radius (au)	4.66 ± 0.11	
	$M \sin i$ ($M_{\rm Jup}$)	6.08 ± 0.13	
	χ^2_ν	7.40	
	rms (s)	6.57	
A2	Orbital period (d)	4647 ± 36	7215 ± 603
	Amplitude (s)	20.2 ± 0.5	23.4 ± 1.9
	Eccentricity	0.19 ± 0.02	0.53 (fixed)
	ω (°)	166 ± 5	190 (fixed)
	T_0 (JD − 240 0000)	$53\,074 \pm 50$	$58\,060 \pm 599$
	Orbital radius (au)	5.59 ± 0.11	7.50 ± 0.50
	$M \sin i$ ($M_{\rm Jup}$)	8.19 ± 0.24	7.07 ± 0.41
	χ^2_ν	0.69	
	rms (s)	2.50	
B1	Orbital period (d)	4728^{+300}_{-250}	
	Amplitude (s)	15.1 ± 1.6	
	Eccentricity	$0.09^{+0.05}_{0.09}$	
	ω (°)	181^{+55}_{-10}	
	T_0 (JD − 240 0000)	$53\,991 \pm 60$	
	Orbital radius (au)	5.66 ± 0.31	
	$M \sin i$ ($M_{\rm Jup}$)	6.05 ± 0.27	
	χ^2_ν	21.2	
	rms (s)	8.00	
B2	Orbital period (d)	4688 ± 177	8377 ± 610
	Amplitude (s)	14.0 ± 2.1	27.9 ± 3.7
	Eccentricity	0.20 ± 0.04	$0.38^{+0.16}_{-0.11}$ (fixed)
	ω (°)	254 ± 12	332 (fixed)
	T_0 (JD − 240 0000)	$53\,640 \pm 116$	$60\,126 \pm 612$
	Orbital radius (au)	5.62 ± 0.22	8.28 ± 0.50
	$M \sin i$ ($M_{\rm Jup}$)	5.65 ± 0.20	7.64 ± 0.12
	χ^2_ν	0.80	
	rms (s)	2.49	

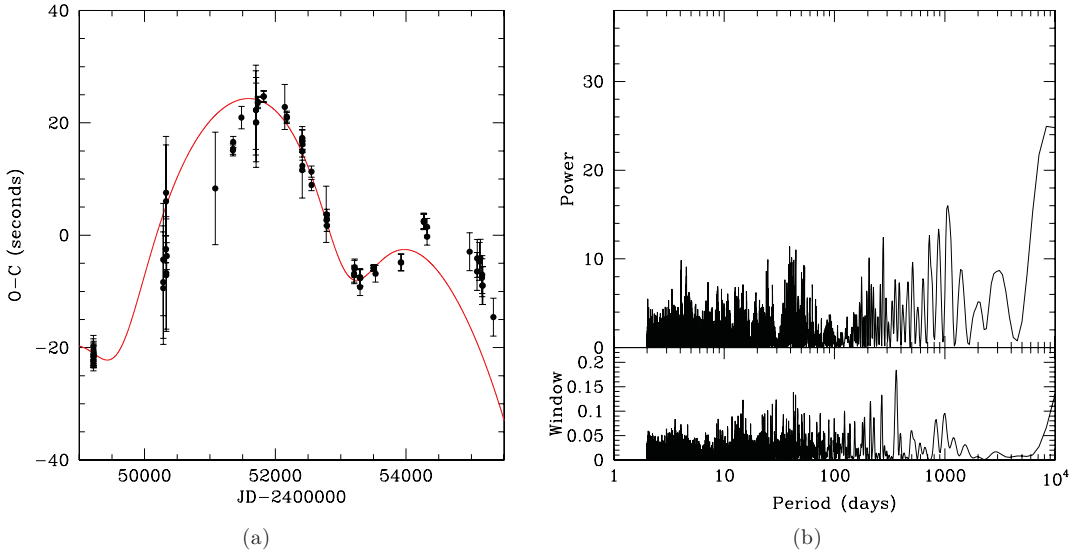

Figure 3. Results of single-planet fit on data with quadratic trend removed (model A1). Left-hand panel: data and model fit for a single planet. The quadratic trend we have removed is superposed on the one-planet Keplerian model (solid line). Right-hand panel: periodogram of residuals after fitting for and removing the dominant signal, a Keplerian orbit with a period of 3538 days. A significant peak is seen at a very long period.

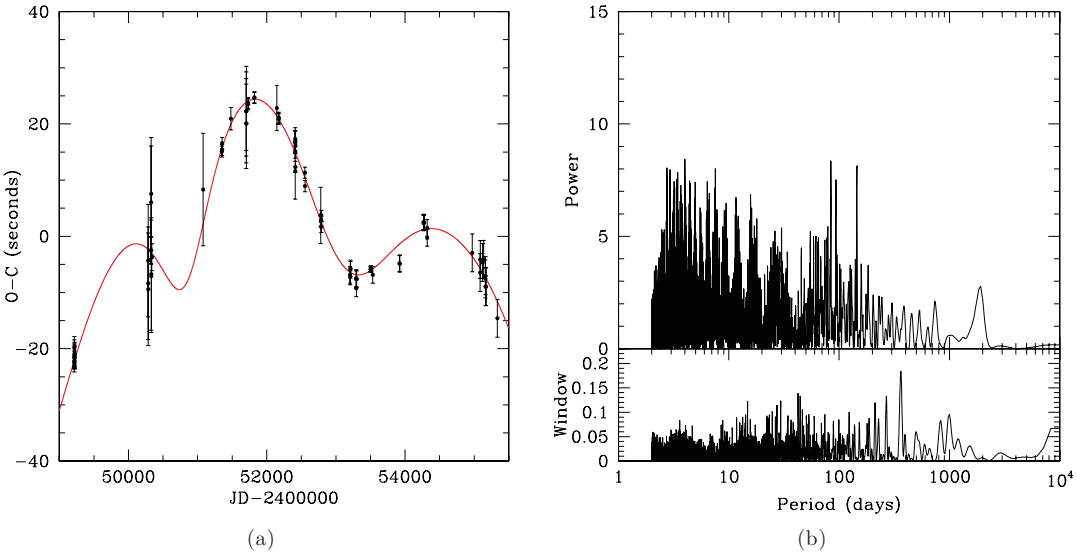

Figure 4. Left-hand panel: two-planet fit (model A2) on data with quadratic trend removed. The quadratic trend we have removed is superposed on the two-planet Keplerian model (solid line). Right-hand panel: periodogram of residuals to this fit. No further significant periods are evident.

7215 days, there remains significant uncertainty in the two-planet fit. In particular, the Keplerian orbit-fitting process failed to converge when the outer planet's eccentricity and periastron argument (ω) were allowed to be free parameters. Hence, the values for these parameters shown in Table 2 were held fixed at the best result from the genetic algorithm. As shown in Fig. 5, these two parameters are almost completely unconstrained. This is not surprising given that the period of the outer planet is larger than the entire length of the data set.

3.2 No quadratic trend

In section, we explore the possibility that the removal of a quadratic trend has confounded the orbit-fitting process by absorbing signal due to a long-period outer planet. Here we repeat the fitting procedures as above, but using the HU Aqr data which have *not* had a quadratic trend subtracted. First, we considered a single planet by performing a periodogram search (Fig. 6), which shows the dominant periodicity to be at 5000 days. However, the standard approach of fitting a Keplerian orbit with GaussFit failed. As the reduced χ^2 of the best-fitting genetic algorithm result was an inordinately high 21.2, we attribute the failure of the least-squares method to the presence of additional signals. In Table 2, we give the best-fitting results for a single planet ('model B1') from 100 000 iterations of the genetic algorithm. The 1σ uncertainties are estimated by noting the change in each parameter required to increase the reduced χ^2 by 1. The dependence of χ^2 on each parameter is shown in Fig. 7. As with the one-planet solution in the previous trial (data which included a quadratic trend), the rms scatter about a one-planet model is quite large at 8.0 s, compared to the mean measurement uncertainty of 2.4 s. The fit and a periodogram of its residuals are shown in Fig. 8; it is clear that one planet is not sufficient here. The highest

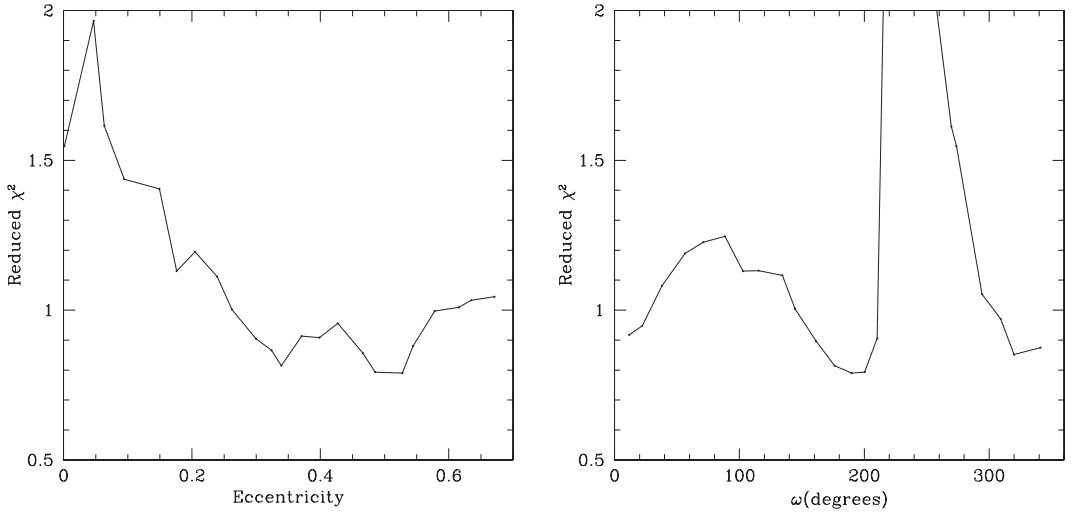

Figure 5. Results of genetic algorithm fitting for two planets (model A2). Left-hand panel: dependence of reduced χ^2 on the outer planet's eccentricity. Right-hand panel: same, but for the outer planet's argument of periastron (ω). These parameters are essentially unconstrained, as nearly the entire allowed range is within 1.0 of the χ^2 minimum.

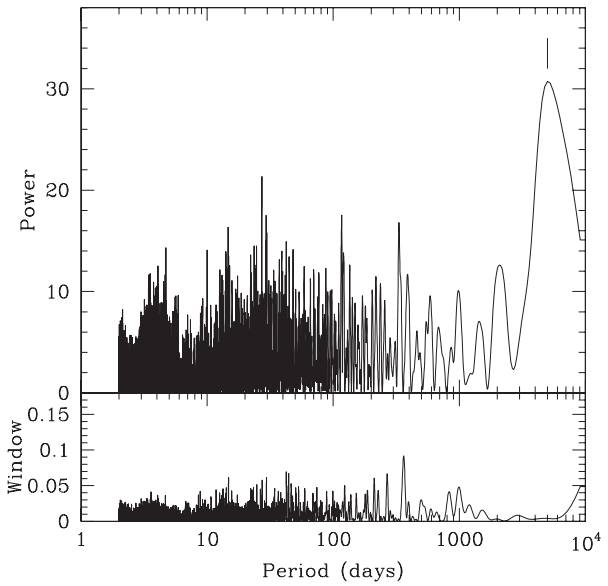

Figure 6. Periodogram of the O − C timing data for HU Aqr, using the raw data (residuals from a linear ephemeris) with *no* additional quadratic trend removed. A strong signal is evident near 5000 days.

periodogram peak is at a period of 2128 days, again with a FAP <0.01 per cent. We thus proceed to fit a second Keplerian orbit.

Again we employ the genetic algorithm to explore the wide and uncertain parameter space for a two-planet model ('model B2'). First we examine the short-period option, as prompted by the periodogram results in Fig. 8. We ran the genetic algorithm for 100 000 iterations, and then attempted a standard least-squares fit on the best result. As with model B1, GaussFit failed to converge on a solution when the eccentricities e and periastron arguments ω of the two planets were allowed to be free parameters. The best-fitting model with a short period for the second planet (actually making it the *inner* of the two planets) resulted in a reduced χ^2 of 4.06 and an rms of 5.97 s. The planetary parameters resulting from this fit are quite similar to those proposed by Qian et al. (2011), with $P_{\rm inner} = 1947 \pm 10$ d and $P_{\rm outer} = 4429 \pm 113$ d. However, this is substantially worse than the two-planet fit from model A2, and also worse than the long-period fit obtained below.

Allowing the genetic algorithm to choose long periods for the second planet, we obtain a far better solution, with a reduced χ^2 of 0.80. The parameters of this fit are given in Table 2 as model B2; this fit and a periodogram of its residuals are shown in Fig. 9. Both models A2 and B2 support a long period for the second planet, so the short-period case discussed briefly above is rejected. Again, the fitting process failed when e and ω for the outer planet were free parameters, so we fixed their values at the best fit from the genetic run (100 000 iterations). Uncertainty estimates are obtained from the plots in Fig. 10; for ω, the χ^2 surface has two minima, and so no formal uncertainty is quoted – this parameter is very poorly constrained due to the long period of the outer planet.

In Qian et al. (2011) and Horner et al. (2011), it was suggested that a third, distant outer planet may be present in the HU Aqr system. However, in light of the results of the two-planet fits given in this section, which feature reduced χ^2 less than 1.0, we see no need to invoke additional bodies to adequately fit the available data.

In summary, our analysis of two slightly different versions of the HU Aquarii data yields evidence for two planets: a moderately well-constrained one at $P = 4647$–4688 d with $e \sim 0.2$ and a somewhat more poorly constrained one at $P = 7215$–8377 d with a poorly constrained but non-zero eccentricity. While the outer planet's period varies by ∼1200d between these two solutions, we note that this represents just a 2σ difference, given the period uncertainties. Hence, there is a long-period outer signal present, even if its period is not well determined.

4 DYNAMICAL ANALYSIS

Following the results detailed above, the observational data yield two distinct two-planet solutions which are essentially identical in terms of their goodness-of-fit criteria. In both solutions, the best-fitting system parameters are significantly different from those given by Qian et al. (2011), whose dynamical stability was studied in some detail in Horner et al. (2011). In that work, the authors

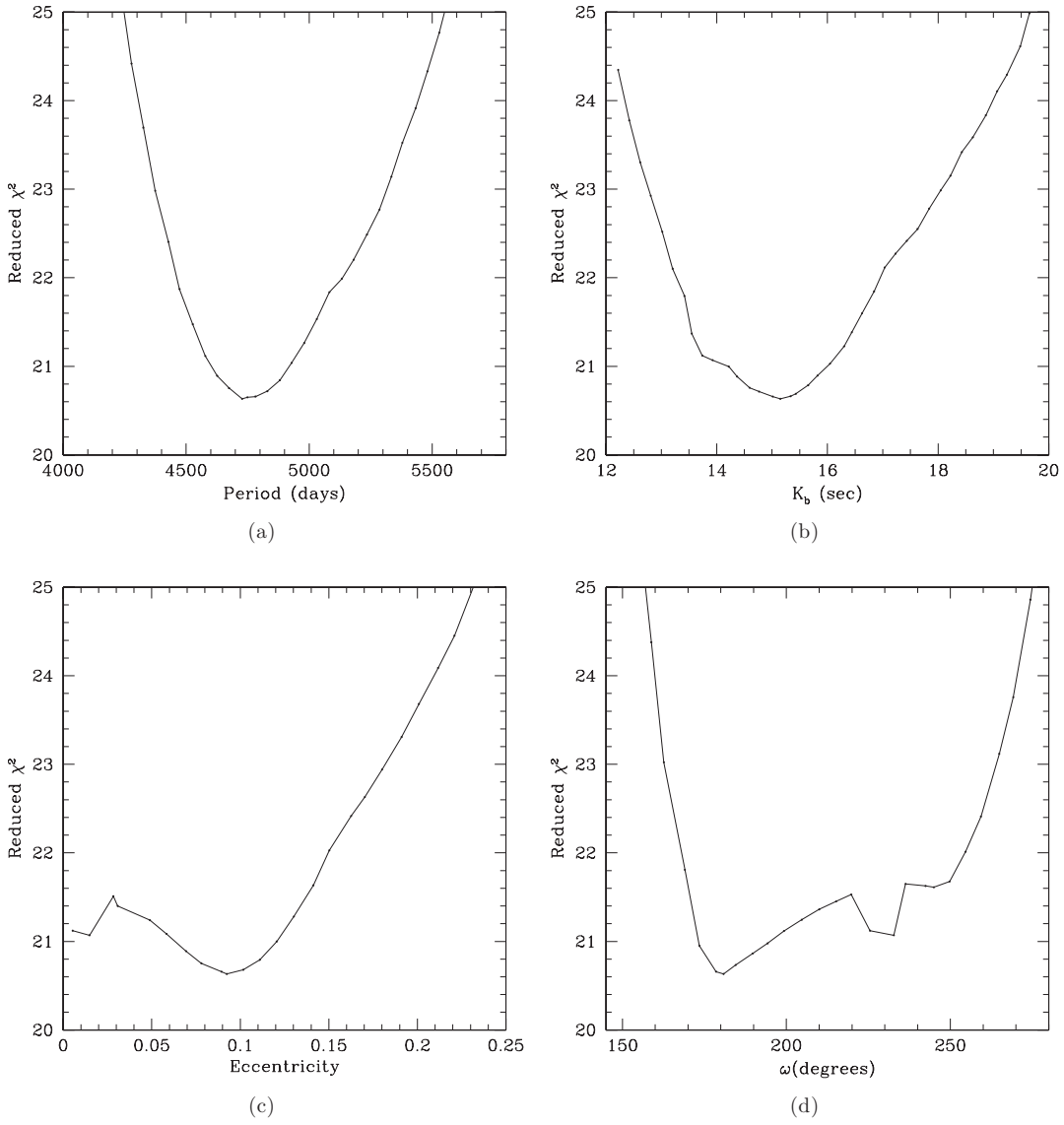

Figure 7. Results of single-planet genetic algorithm fit for HU Aqr (model B1). Each panel shows the dependence of reduced χ^2 on a particular planetary parameter. The uncertainty of each parameter is estimated by the range over which the reduced χ^2 increases by 1 from the minimum.

argued that the extreme levels of dynamical instability displayed by the planetary system provided firm evidence that, at the very least, the true parameters of the planets in the system were greatly different from those obtained through the analysis of Qian et al. (2011).

How do the new solutions for the proposed HU Aqr planets stand up to the same test? In order to closely examine the dynamical stability of the newly proposed solutions, we followed Horner et al. (2011) and Marshall et al. (2010) and performed highly detailed dynamical simulations of the potential planetary systems. Such simulations serve as a critically important additional test, since the algorithms used to this point include no physics; rather, the Keplerian fitting methods are simply seeking a lowest χ^2 solution regardless of the physicality of the resulting system parameters.

As in Horner et al. (2011), we used the hybrid integrator within the *N*-body dynamics package MERCURY (Chambers 1999) to perform our integrations. For the two scenarios in question (models A2 and B2), we created 50625 test planetary systems. In each case, we followed our earlier work, and kept the initial orbit of the innermost planet fixed at its nominal best-fitting value. The initial orbit of the outermost planet was then varied systematically in semimajor axis a, eccentricity e and mean anomaly M, such that a total of 50 625 unique solutions were tested. For our tests of each of the two models, 45 initial values of a were tested, spread evenly across the full $\pm 3\sigma$ error range in that parameter. Similarly, 45 initial values of e were tested in each case, with 25 different M being considered for each a–e pairing. For model A2, in which the e of the outermost planet was unconstrained, we tested eccentricities ranging between 0.005 and 0.995, whilst for model B2, the tested e values were spread across the full $\pm 3\sigma$ errors given in Table 2.

As in Horner et al. (2011), we followed the dynamical evolution of each test system for a period of 100 Myr and recorded the times at which either of the planets was removed from the system. Planets were removed if they collided with one another, hit the central body or reached a barycentric distance of 100 au.

The results of our dynamical integrations can be seen in Figs 11 and 12. The 3σ region around the nominal orbits in a–e space is clearly highly dynamically unstable. As was seen in the dynamical

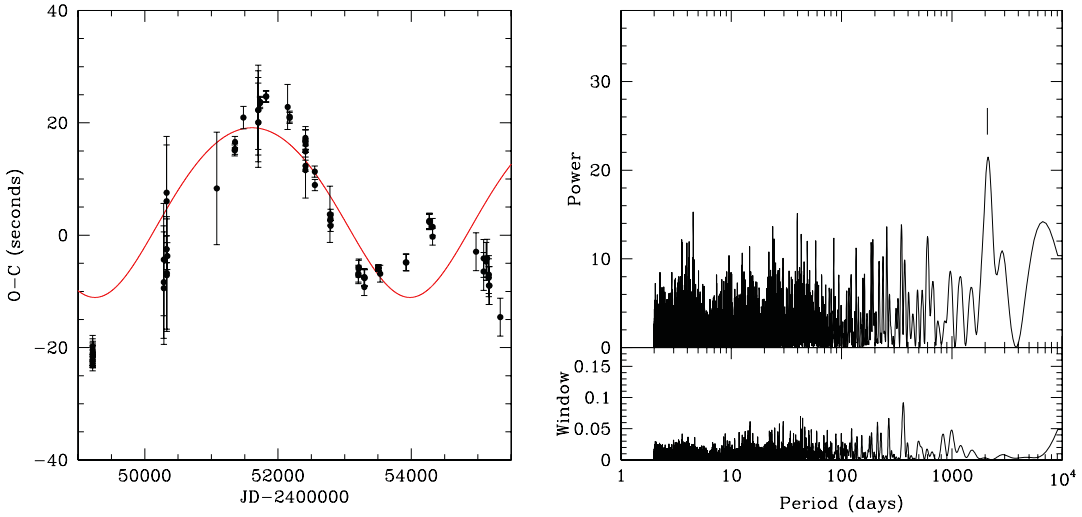

(a) (b)

Figure 8. Results of single-planet fit for HU Aqr (model B1). Left-hand panel: data and model fit for a single planet. Clearly a single planet is inadequate to fit these data. Right-hand panel: periodogram of residuals after fitting for and removing the dominant signal, a Keplerian orbit with a period of 4728 days. A significant peak is seen near 2100 days.

study of the planetary system proposed by Qian et al. (2011), low-eccentricity orbital solutions that keep the planets separated at all times by at least three Hill radii offer some moderate increase in the potential stability of the system. We note that these regions lie far from the central 1σ of the error ellipse. Furthermore, a fit with the outer planet's period and eccentricity fixed in this stable region has a reduced χ^2 of 14.9, far worse than the best-fitting results given in Table 2.

Much as was the case for the planetary system as proposed by Qian et al. (2011), we therefore find that both of the best-fitting models detailed above (models A2 and B2) fail to stand up to dynamical scrutiny. We find that the resulting dynamical instabilities make it exceedingly unlikely that the eclipse-timing variations observed for HU Aqr are truly the result of perturbations from planetary-mass objects in the system. It seems reasonable, therefore, to examine more closely whether any other effects could cause timing variations of an appropriate periodicity and scale in such eclipsing polar systems.

5 ALTERNATIVES TO THE PLANET HYPOTHESIS

There are many causes of variability, spanning time-scales from seconds to years, which are inherent to the nature of CVs. All of these mechanisms may have an observable impact on the variation of the O − C curve, which may act to dilute, obscure or mimic a signal that would otherwise be attributable to the presence of exoplanet(s).

At the time-scale considered here (i.e. thousands of days) the most likely source of the observed variation in the O − C curve is the

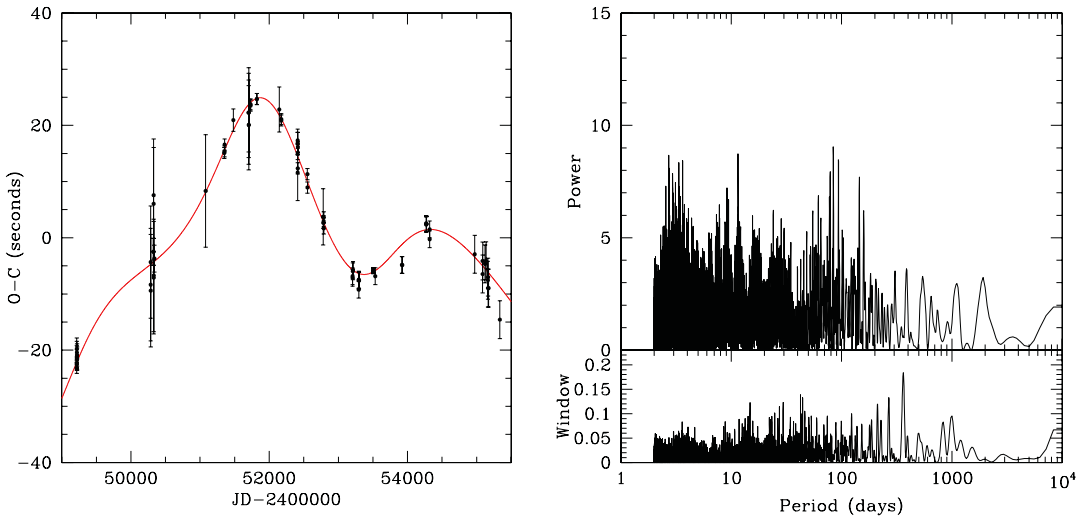

(a) (b)

Figure 9. Left-hand panel: two-planet fit (model B2) to the observed data with no quadratic trend removed. Right-hand panel: periodogram of residuals to this fit. No further significant periods are evident.

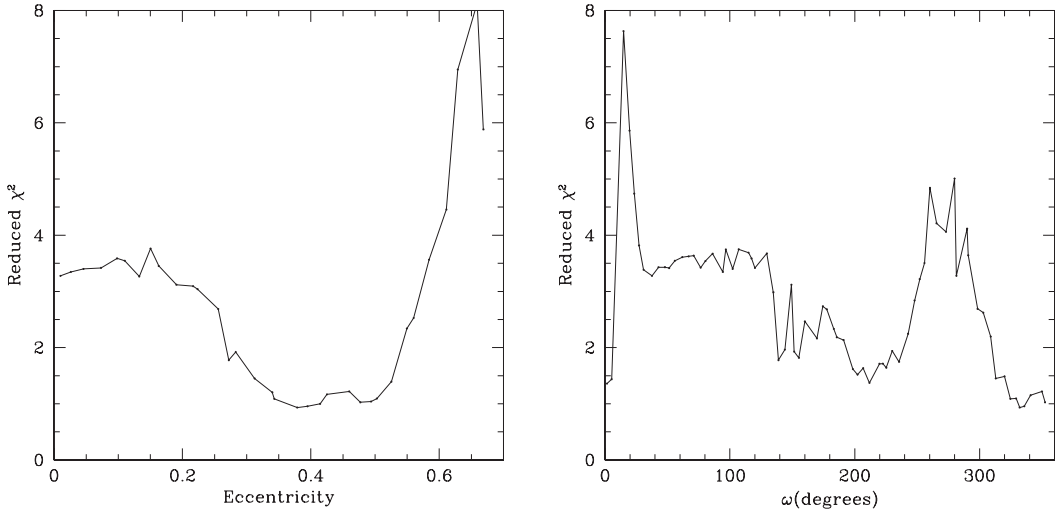

(a) (b)

Figure 10. Results of genetic algorithm fitting for two planets (model B2). Left-hand panel: dependence of reduced χ^2 on the outer planet's eccentricity. Right-hand panel: same, but for the outer planet's argument of periastron (ω). This parameter displays two minima, and so is very poorly constrained by the available data.

secondary star in the system, the M dwarf. With a rotation period of the order of a few hours (the result of it being tidally locked in its rotation about the primary, the white dwarf), the dynamo effect in the secondary could be large. Assuming that the stars in such systems have a magnetic cycle similar to the Sun's double-peaked 22-year cycle, then their angular momentum distribution will change over time. This will have the effect of altering the shape of the secondary, which in turn affects the gravitational attraction between the primary and secondary – and hence the orbital period (Warner 1988; Applegate 1992).

This effect has already been observed in several CVs. Examples include U Gem, which displays a ∼1 min variation in orbital period over an 8-year time-scale (Eason et al. 1983), EX Dra, whose period varies by 1.2 min over approximately 4 years (Baptista, Catalán & Costa 2000) and EX Hya, whose period is modulated on a time-scale of approximately 17.5 years (Hellier & Sproats 1992).

On the question of planetary survivability, Qian et al. (2011) mentioned that a gas giant planet could survive the planetary nebula stage, so long as it was located beyond orbital distances of about 3 au (Villaver & Livio 2007; Kunitomo et al. 2011). However, to make it to the planetary nebula phase, the planet must first survive the asymptotic giant branch (AGB) phase. A normal AGB star with a main-sequence mass of 5 $M_\odot$ (extrapolated from the white dwarf mass of 0.88 $M_\odot$) is expected to reach a radius of 5.25 au, enveloping both of the postulated planets from Qian et al. (2011). A planet entering the envelope of an AGB star would clearly have

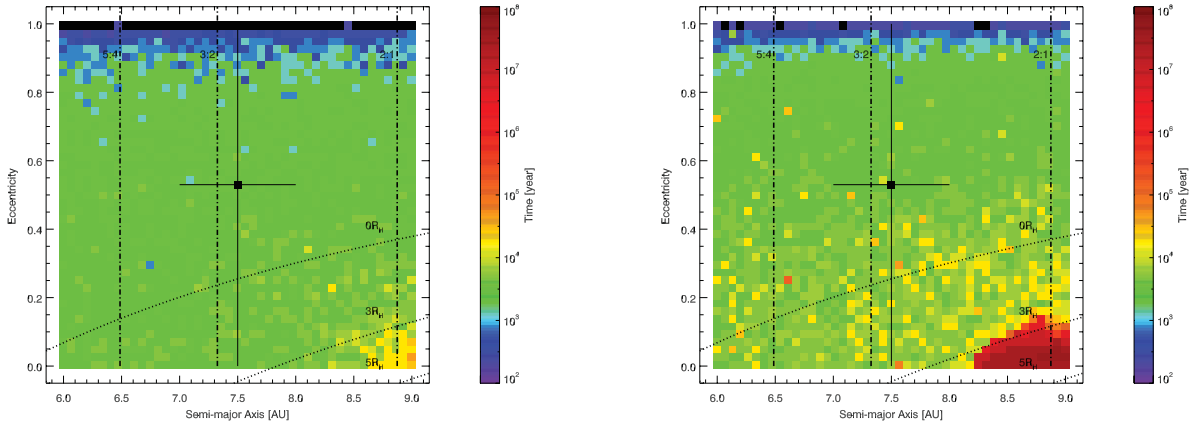

(a) (b)

Figure 11. Left-hand panel: median lifetime of the outermost planet in the HU Aqr system, based on the orbits fitted by model A2, as a function of the planet's semimajor axis a and eccentricity e. The lifetime shown in each square is the median of the 25 distinct runs (each of which had the planet start at a different initial mean anomaly M). In both panels, the vertical dashed lines indicate relevant mean-motion resonances. This panel reveals that the whole phase space of potential orbits described in model A2 is highly dynamically unstable, with median lifetimes typically much less than 10^5 yr. Right-hand panel: same as the left-hand panel, except that the mean, rather than the median, of the 25 initial mean anomaly values is calculated for each bin across the plot. Whereas the left-hand panel clearly showed the overall lack of stability of the plausible orbital solutions given by model A2, plotting the *mean* lifetimes of each bin reveals that, for a small region of orbital space for which the outermost planet could approach no closer than $3R_H$ to the innermost planet, some fraction of the tested orbits were dynamically stable on much longer time-scales.

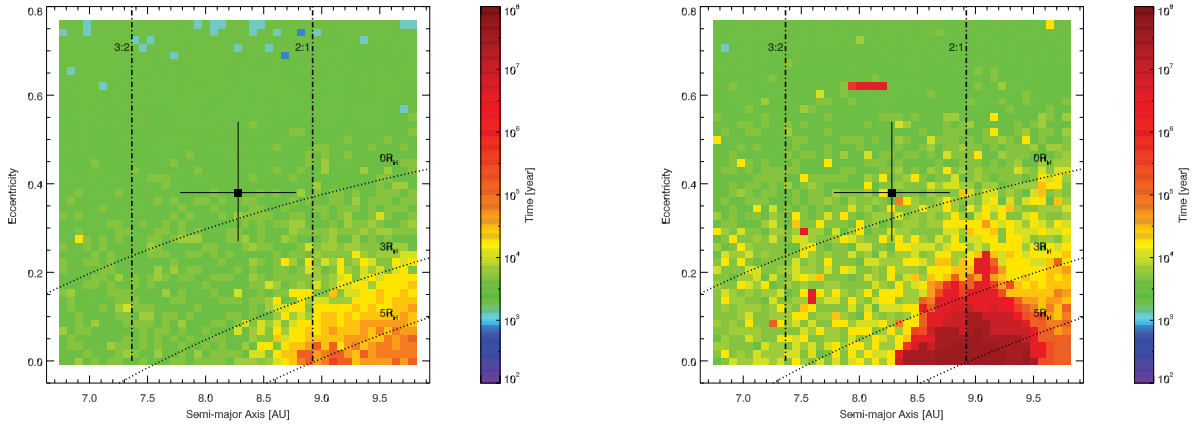

Figure 12. Left-hand panel: median lifetime of the outermost planet in the HU Aqr system, based on the orbits fitted by model B2, as a function of the planet's semimajor axis a and eccentricity e, as described above. In both panels, the vertical dashed lines indicate relevant mean-motion resonances. The great bulk of the tested a–e phase space is highly dynamically unstable. Right-hand panel: same as the left-hand panel, except that the mean, rather than the median, of the 25 initial mean anomaly values is calculated for each bin across the plot. As was the case for the results of model A2, this reveals that a small fraction of orbits tested can display long-term dynamical stability, though such orbits remain in the minority.

very little chance of surviving. Planets orbiting post-main-sequence stars are thought to be either survivors of the planetary nebula or supernova phase (Colgate 1970; Postnov & Prokhorov 1992; Veras et al. 2011), or formed from a second phase of planet formation, accreting from some of the material shed by the primary star (Tavani & Brookshaw 1992; Phinney & Hansen 1993; Hansen, Shih & Currie 2009). This 'second-generation' planet formation scenario was explored after the discovery of the terrestrial-mass planets orbiting pulsars (Wolszczan & Frail 1992). However, the mechanism by which Jupiter-mass planets could form in such an evolved system is not currently clear.

6 SUMMARY AND CONCLUSIONS

We have revisited the work of Qian et al. (2011), who reported that timing variations in the mutual eclipses between the primary and secondary components of the HU Aqr system were evidence that there were at least two Jupiter-mass planetary companions orbiting around the two central stars.

In this work, we applied the key tools used in the detection of planets around main-sequence stars through the radial-velocity technique to the data used by Qian et al. (2011). Our analysis resulted in two distinct two-planet fits which could, in theory, explain the observed timing variations.

Our derived orbital solutions differ significantly from those presented in that earlier work, but still fall prey to the same dynamical drawback. Simply put, the planets necessary in order to explain the eclipse-timing variations prove dynamically unstable on time-scales so short as to seem unfeasible.

Our results therefore suggest that some other mechanism must instead be invoked in order to explain the observed variations. The most likely candidate, based on earlier studies of eclipsing polar systems, is that the observed variations are the result of the interaction between the magnetic fields of the stars in the course of their stellar cycles. Such variations have been observed in a number of eclipsing polar systems in the past, and would be expected to yield variations on the scale observed, over similar time-scales.

In light of these results, it would seem prudent in future to consider such behaviour as a potential source of signals that could mimic the presence of planets orbiting CV stars. Rigorous dynamical testing of any planetary system resulting from the analysis of transit timing data for such stars should become a key component of the analytical process. These tests will prove critical in distinguishing between CVs which might plausibly host such interesting planetary systems, and those in which such planets are all but impossible.

ACKNOWLEDGMENTS

JH and CGT gratefully acknowledge the financial support of the Australian government through ARC Grant DP0774000. RAW is supported by a UNSW Vice-Chancellor's Fellowship. JPM is partly supported by Spanish grant AYA 2008/01727, thanks Eva Villaver for constructive discussions of planet survivability and gratefully acknowledges Maria Cunningham for funding his collaborative visit to UNSW.

REFERENCES

Applegate J. H., 1992, ApJ, 385, 621
Baptista R., Catalán M. S., Costa L., 2000, MNRAS, 316, 529
Beuermann K. et al., 2010, A&A, 521, L60
Chambers J. E., 1999, MNRAS, 304, 793
Cochran W. D., Endl M., Wittenmyer R. A., Bean J. L., 2007, ApJ, 665, 1407
Colgate S. A., 1970, Nat, 225, 247
Eason E. L. E., Africano J. L., Klimke A., Worden S. P., Quigley R. J., Rogers W., 1983, PASP, 95, 58
Hansen B. M. S., Shih H.-Y., Currie T., 2009, ApJ, 691, 382
Hellier C., 2001, Cataclysmic Variable Stars. Springer, Berlin
Hellier C., Sproats L. N., 1992, Inf. Bull. Var. Stars, 3724, 1
Horner J., Marshall J. P., Wittenmyer R. A., Tinney C. G., 2011, MNRAS, L280
Jefferys W. H., Fitzpatrick M. J., McArthur B. E., 1987, Celest. Mech., 41, 39
Kunitomo M., Ikoma M., Sato B., Katsuta Y., Ida S., 2011, ApJ, 737, 66

Kürster M., Schmitt J. H. M. M., Cutispoto G., Dennerl K., 1997, A&A, 320, 831
Lomb N. R., 1976, Ap&SS, 39, 447
Marshall J., Horner J., Carter A., 2010, Int. J. Astrobiol., 9, 259
Phinney E. S., Hansen B. M. S., 1993, in Phillips J. A., Thorsett J. E., Kulkarni S. R., eds, Proc. Conf. California Institute of Technology, Vol. 36, Planets Around Pulsars. Astron. Soc. Pac., San Francisco, p. 371
Postnov K. A., Prokhorov M. E., 1992, A&A, 258, L17
Potter S. B. et al., 2011, MNRAS, 416, 2202
Qian S.-B., Liao W.-P., Zhu L.-Y., Dai Z.-B., 2010, ApJ, 708, L66
Qian S.-B. et al., 2011, MNRAS, 414, L16
Scargle J. D., 1982, ApJ, 263, 835
Schwarz R., Schwope A. D., Vogel J., Dhillon V. S., Marsh T. R., Copperwheat C., Littlefair S. P., Kanbach G., 2009, A&A, 496, 833
Tavani M., Brookshaw L., 1992, Nat, 356, 320
Tinney C. G., Wittenmyer R. A., Butler R. P., Jones H. R. A., O'Toole S. J., Bailey J. A., Carter B. D., Horner J., 2011, ApJ, 732, 31
Veras D., Wyatt M. C., Mustill A. J., Bonsor A., Eldridge J. J., 2011, MNRAS, 417, 2104
Villaver E., Livio M., 2007, ApJ, 661, 1192
Warner B., 1988, Nat, 336, 129
Wolszczan A., Frail D. A., 1992, Nat, 355, 145

This paper has been typeset from a TEX/LATEX file prepared by the author.